Supplementary Information (SI) for Journal of Materials Chemistry A.

Supporting Information for

Pinning and Elongating of Electric Treeing Induced by Wrinkled Nanosheets in Polymer Dielectrics towards Significantly Enhanced High-temperature Energy Storage Performance

Xuyuan Fan[a], Linwei Zhu[a], Zelong Chang[a], Qingyang Tang[a], Davoud Dastan[b], Runhua Fan[c], Zhicheng Shi[a,]*

[a] *School of Materials Science and Engineering, Ocean University of China, Qingdao 266100, China*

[b] *Department of Materials Science and Engineering, Cornell University, Ithaca, NY 14850, USA*

[c] *College of Ocean Science and Engineering, Shanghai Maritime University, Shanghai 201306, P. R. China.*

*Corresponding author: Zhicheng Shi

E-mail: zcshi@ouc.edu.cn (Z.Shi)

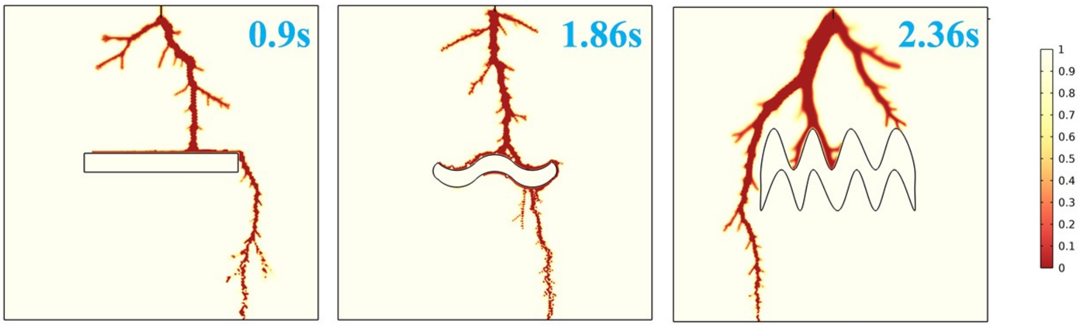

Figure S1 Simulated breakdown paths of flat (left), low-curvature (middle), and high-curvature (right) nanosheets

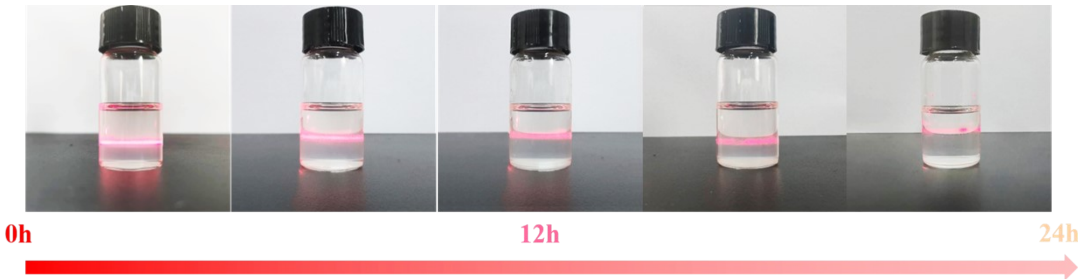

Figure S2 The Tyndall Effect of WAO Solution (NMP as Solvent)

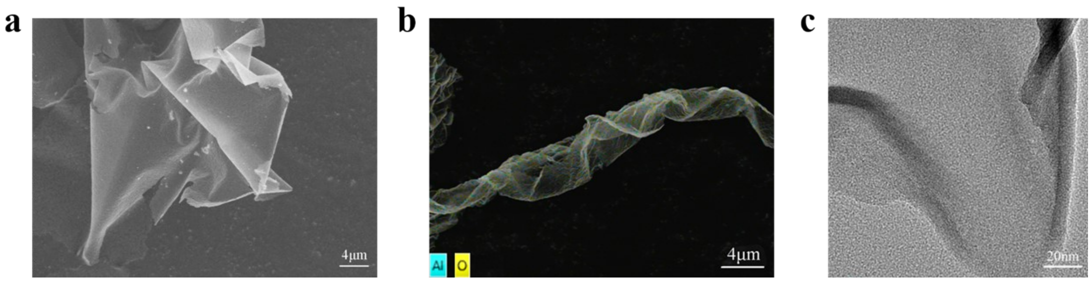

Figure S3 (a) SEM; (b) EDX and (c) high magnification TEM image of wrinkled nanosheets

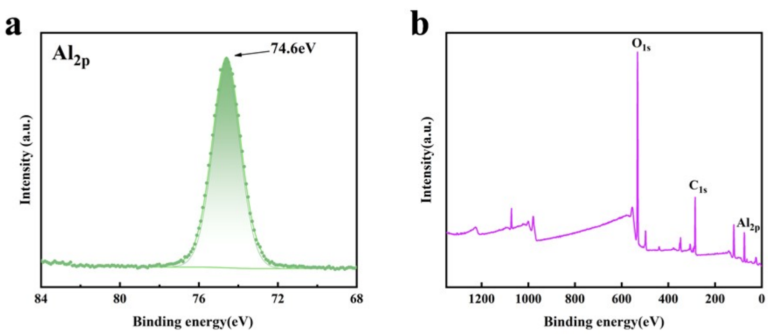

Figure S4 XPS image of wrinkled Al_2O_3 nanosheets

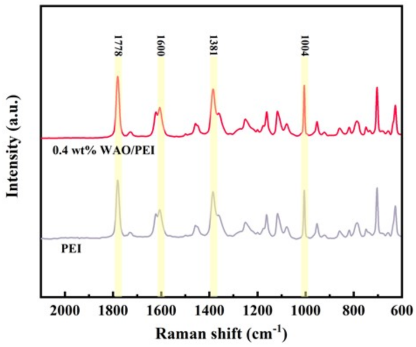

Figure S5 Raman spectra of pure PEI and 0.4 wt% WAO/PEI films

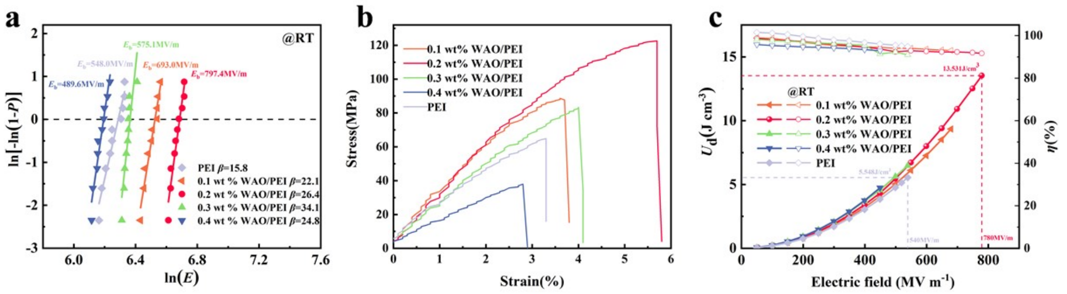

Figure S6 (a) The breakdown strength; (b) Representative tensile strengths; (c) Energy storage density of pure PEI and 0.1- 0.4 wt% WAO/PEI films at room temperature

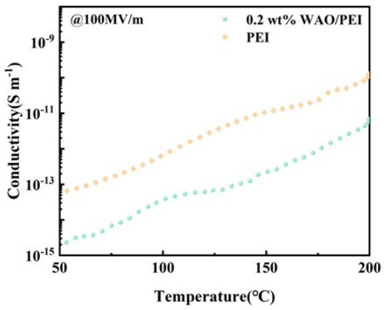

Figure S7 The temperature-dependent conductivity of pure PEI and 0.2 wt% WAO/PEI composite films

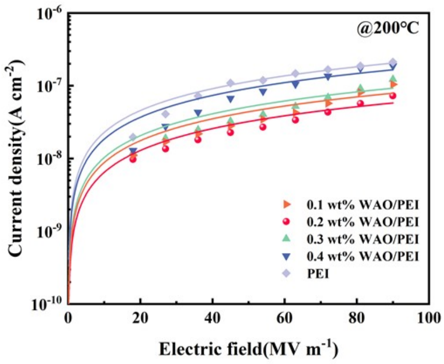

Figure S8 Leakage current density of pure PEI and 0.1-0.4wt% composite films at 200℃

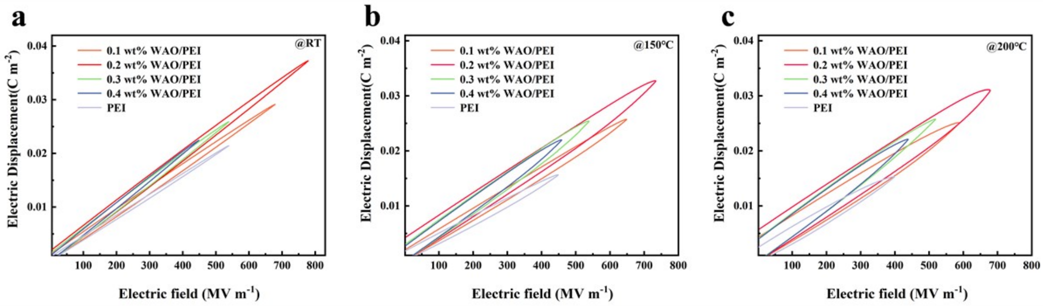

Figure S9 *D-E* loops of WAO/PEI at (a) RT, (b) 150 °C, and (c) 200 °C

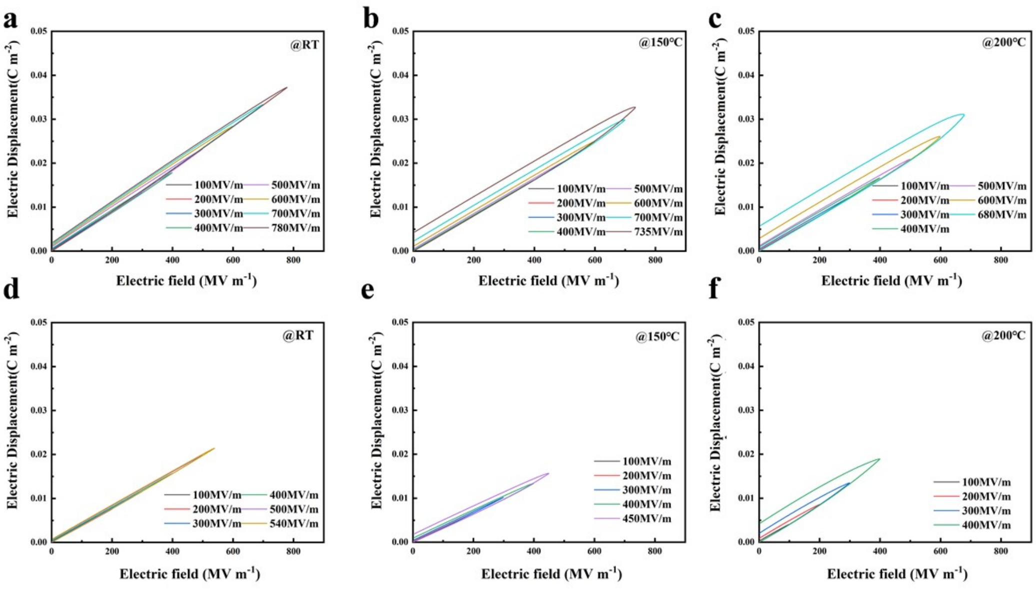

Figure S10 *D-E* loops of pure PEI and 0.2 wt% WAO/PEI composite films under different electric fields at room temperature, 150 ℃, and 200 ℃

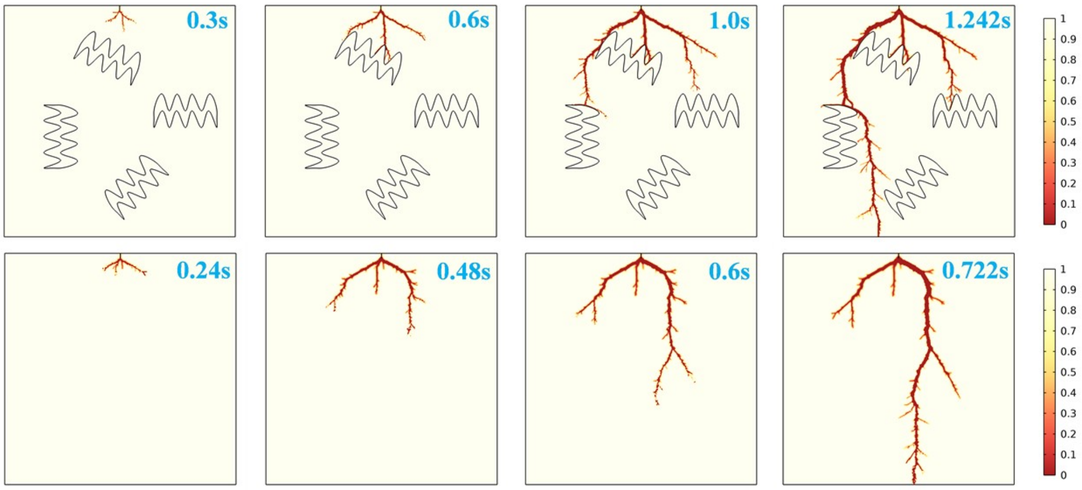

Figure S11 Breakdown path simulation of WAO/PEI composites (top) and PEI (bottom) via COMSOL software

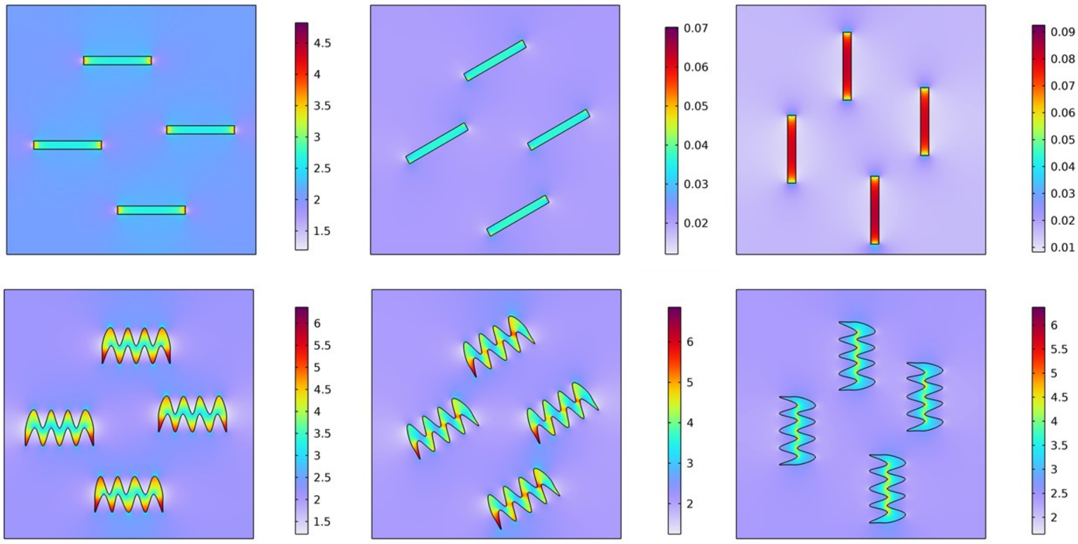

Figure S12 Polarization of flat nanosheets (top) and wrinkled nanosheets (bottom) with different orientations

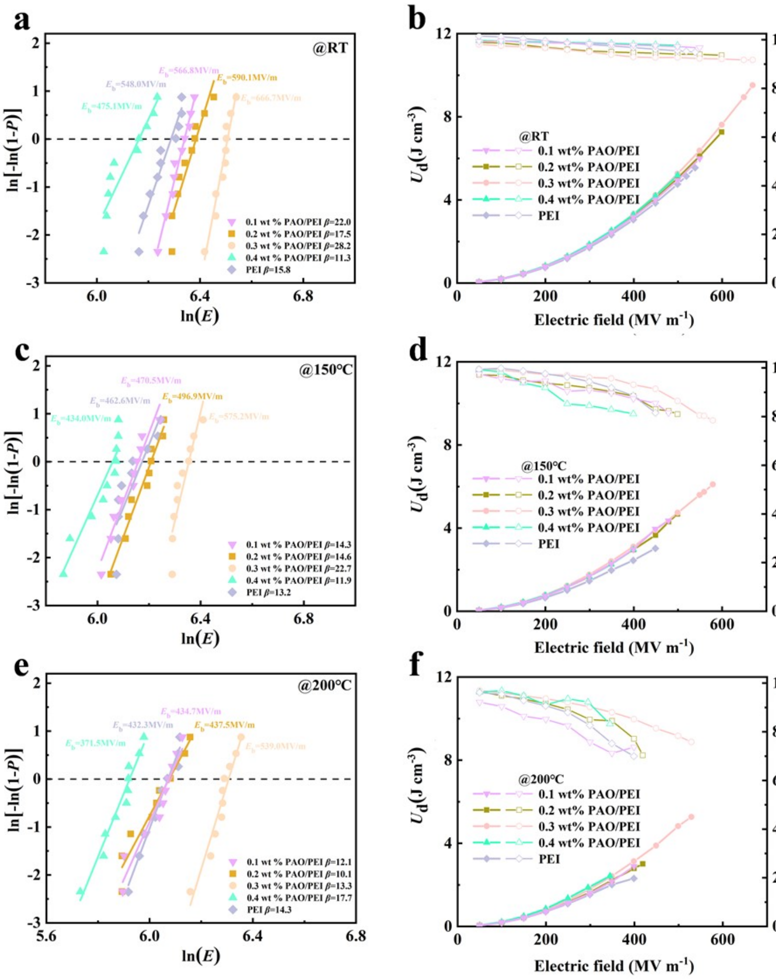

Figure S13 Breakdown strength and energy storage density of PAO/PEI composites at room temperature, 150 °C, 200 °C

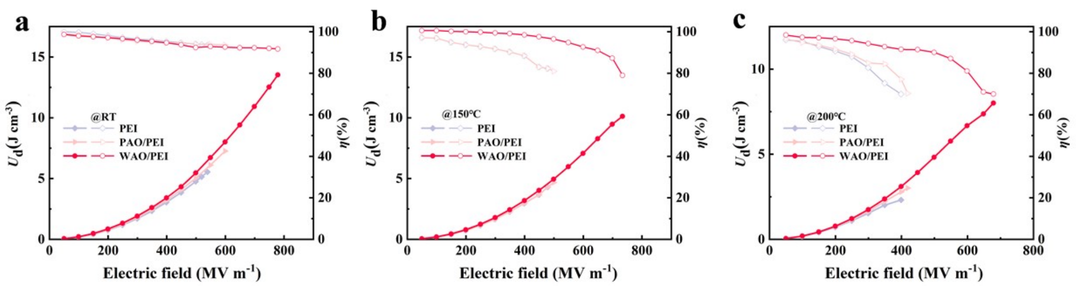

Figure S14 Energy storage density of pure PEI、0.2 wt% PAO/PEI and 0.2 wt% WAO/PEI composites at room temperature, 150 °C, 200 °C

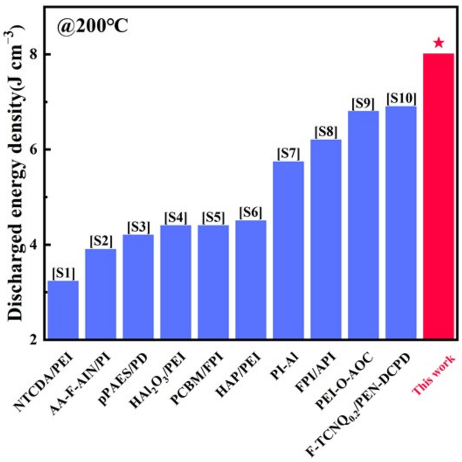

Figure S15 The maximum discharge energy density at 200℃ was compared to the previously published discharge energy density of a high temperature polymer composite film. [S1-S10]

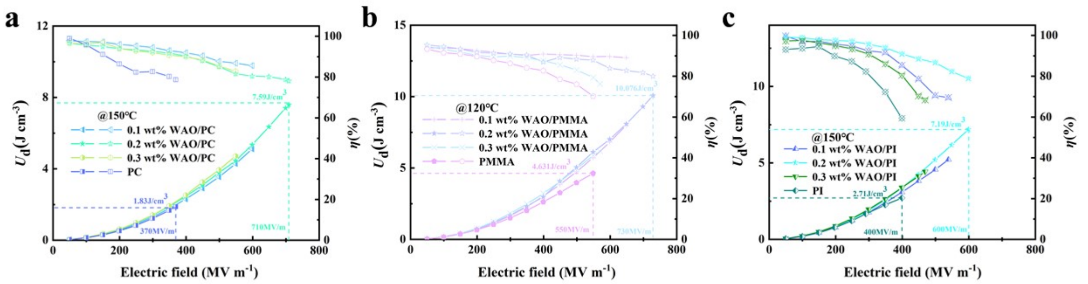

Figure S16 Energy storage properties of wrinkled alumina incorporated into PC, PMMA, and PI at elevated temperatures

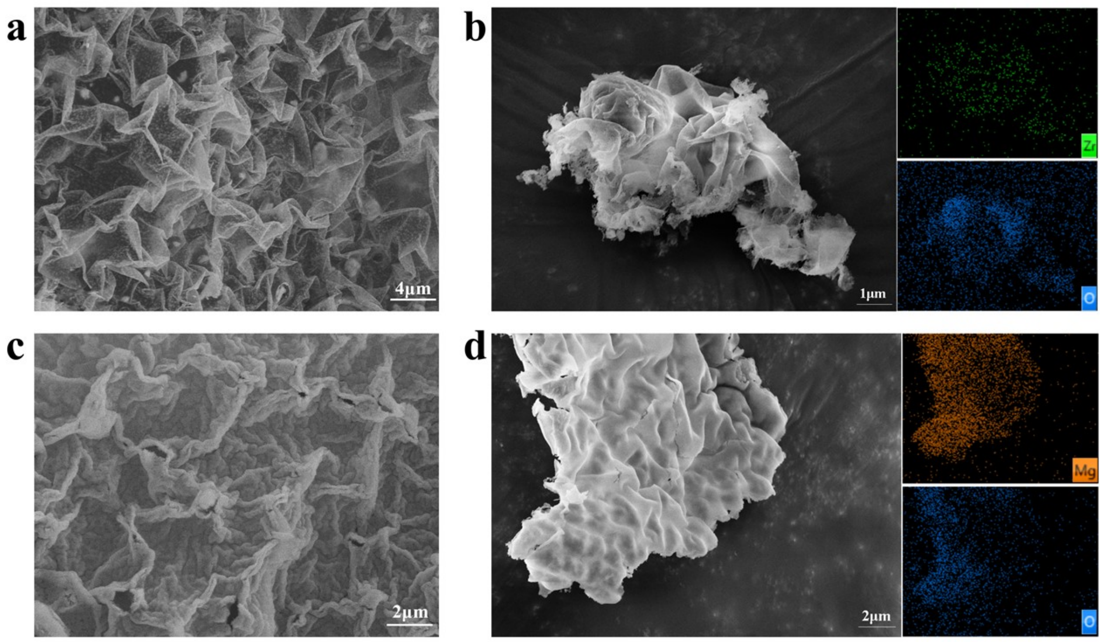

Figure S17 SEM image of a) wrinkled MgO nanosheets b) wrinkled ZrO_2 nanosheets

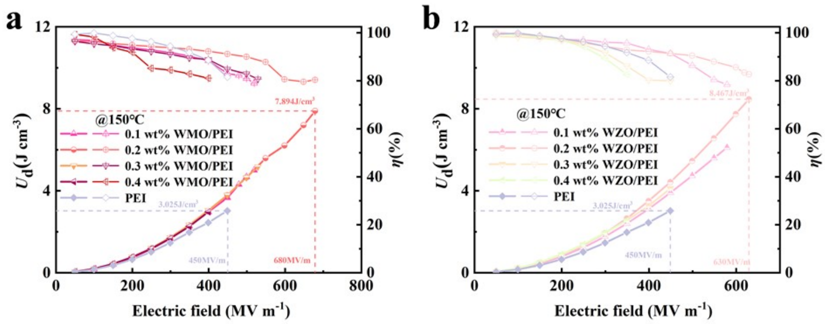

Figure S18 Energy storage properties of wrinkled magnesium oxide and zirconium oxide produced by a similar method incorporating PEI at elevated temperatures

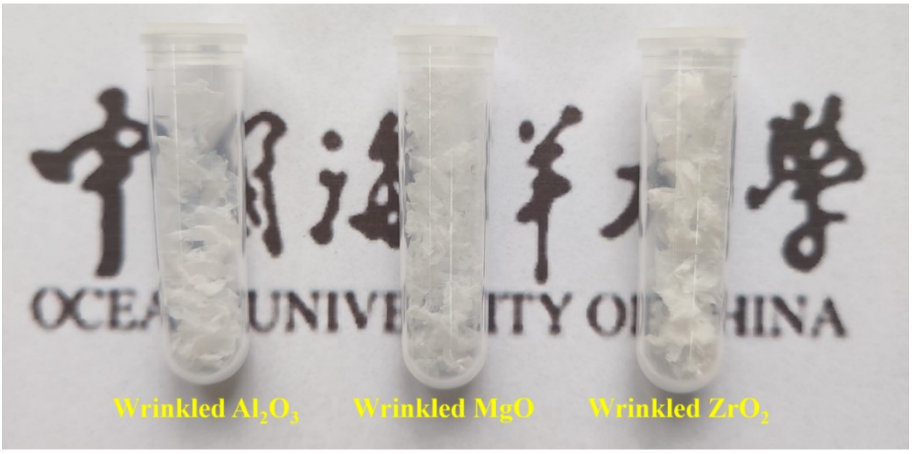

Figure S19 Macroscopic morphology of wrinkled Al_2O_3, MgO and ZrO_2

Table S1 EDX mapping elemental analyses showed the mass fractions of the elements Al and O

Elements	Signal Type	Wt%	Wt% Sigma	At%
O	EDS	50.43	0.69	63.1
Al	EDS	49.57	0.69	36.9

Table S2 Charge carier trap depth (*E*, eV) and density (*Q*, nC) determined by TSDC curves of pure PEI and composite films

Film	Peak 1		Peak 2	
	***E*(eV)**	***Q*(nC)**	***E*(eV)**	***Q*(nC)**
WAO/PEI	2.07	64.08	1.29	44.20
PEI	1.45	136.68	0	0

References

[S1] B. Zhang, X. m. Chen, Z. Pan, P. Liu, M. Mao, K. Song, Z. Mao, R. Sun, D. Wang, S. Zhang, *Adv. Funct. Mater.* 2022, **33**, 2210050.

[S2] F. Wang, H. Wang, X. Shi, C. Diao, C. Li, W. Li, X. Liu, H. Zheng, H. Huang, X. Li, *Chem. Eng. J.* 2024, **485**, 149972.

[S3] J Ding, Y Zhou, W Xu, F Yang, D Zhao, Y Zhang, Z Jian, Qing Wang, *Nano-Micro Lett.* 2023, **16**, 59-67.

[S4] M. Yang, Y. Zhao, Z. Wang, H. Yan, Z. Liu, Q. Li, Z.-M. Dang, *Energy Environ.Sci.* 2024, **17**, 1592-1602.

[S5] W. Ren, M. Yang, L. Zhou, Y. Fan, S. He, J. Pan, T. Tang, Y. Xiao, C. W. Nan, Y. Shen, *Adv. Mater.* 2022, **34**, 2207421.

[S6] M. Yang, F. Yuan, W. Shi, W. Ren, M. Guo, C. Ouyang, L. Zhou, N. Sun, Y. Xiao, E. Xu, X. Zhang, Y. Wei, X. Deng, C. Nan, X. Wang, Y. Shen, *Adv. Funct. Mater.* 2023, **33**, 2214100.

[S7] W. Ren, M. Yang, M. Guo, L. Zhou, J. Pan, Y. Xiao, E. Xu, C. Nan, Y. Shen, *Energy Storage Mater.* 2024, **65**, 103095.

[S8] M. Liu, J. Song, H. Qin, S. Qin, Y. Zhang, W. Xia, C. Xiong, F. Liu, *Adv. Funct. Mater.* 2024, **34**, 2313258.

[S9] M. Yang, S. Wang, J. Fu, Y. Zhu, J. Liang, S. Cheng, S. Hu, J. Hu, J. He, Q. Li, *Adv. Mater*. 2023, **35**, 2301936.

[S10] J. Chen, Z. Pei, Y. Liu, K. Shi, Y. Zhu, Z. Zhang, P. Jiang, X. Huang, *Adv. Mater.* 2023, **35**, 2306562.